ORIGINAL ARTICLE

Morphometric and morphological evaluation of temporozygomatic suture anatomy in dry adult human skulls

Kemal Emre Özen[1] · Hatice Kübra Yeşil[1] · Mehmet Ali Malas[1]

Abstract

This study aims to evaluate the position, morphometric, and morphological features of the temporozygomatic suture (TZS) located on the zygomatic arch (ZA) in dry adult human skulls. Thirty-two crania were evaluated. Measurements for the TZS were carried out using the ImageJ software. Morphometric measurements were carried out bilaterally in 23 crania and unilaterally in 9 crania (right: 4, left: 5). A total of 55 TZSs were analyzed. Localization of the TZS was determined according to the reference landmarks on the ZA. Morphologic features of the TZS evaluated in terms of "joint shape type" and "suture margin pattern". Descriptive statistics of the morphometric and morphologic variables were calculated. A statistically significant difference between the right and left sides was observed for the localization of the TZS ($p < 0.05$). TZS is located more anteriorly on the left side than the right side. Based on the "joint shape type", four types of TZS were observed: Type 1 (angular) (34.55%), Type 2 (curvy) (34.55%), Type 3 (oblique) (14.55%), Type 4 (horizontal) (16.36%). Based on the "suture margin pattern", five types of TZS were observed: Type A (linear) (12.73%), Type B (denticulate) (34.55%), Type C (serrated) (23.64%), Type D (mixt) (21.82%), Type E (fused) (7.27%). No significant association between the type and lateralization was found for both morphologic classifications. To the best of our knowledge, this is the first published report regarding the localization and morphologic classification of the TZS in adult human crania. Considering the TZS with its morphometric and morphological features may contribute to clinical or forensic medical evaluations.

Keywords Temporozygomatic suture · Zygomatic arch · Joint shape type · Morphology · Morphometry · Suture margin pattern · Zygomaticotemporal suture

Introduction

The zygomatic arch (ZA) is a bridge-like bony structure constituted by the zygomatic bone's temporal process and the temporal bone's zygomatic process. It borders the lower lateral side of the temporal fossa. The temporal process is shorter compared to the zygomatic process. The processes create the temporozygomatic suture (TZS, Latin: sutura temporozygomatica). The lateral surface of the ZA is convex and can be easily palpated beneath the skin (Gleeson 2016). ZA is a remarkable component of face morphology (Cui and Leclercq 2017). ZA is open to traumas owing to its superficial position. ZA and zygomatic bone can be fractured by the lateral impacts. Structures such as ZA, which participate in the formation of facial features, are examined in forensic medicine by analyzing the digital morphometry or biogeographical profiles (Sholts et al. 2011).

Zygomaticomaxillary suture is one of the three joints of the zygomatic bone. The pattern of this suture and morphometric types were evaluated to differentiate the crania of American Indians and Europeans (Sholts and Wärmländer 2012). Angled sutures are overrepresented among American Indians, while curved sutures are predominantly observed in Europeans (Sholts and Wärmländer 2012). In the literature, a combination of the metric and non-metric methods is recommended to analyze the racial or geographical origin of the crania (Sholts and Wärmländer 2012).

✉ Kemal Emre Özen
  kemalemre9870@yahoo.com; kemalemre.ozen@ikcu.edu.tr

  Hatice Kübra Yeşil
  hkubrayesil@gmail.com

  Mehmet Ali Malas
  mehmetalimalas@gmail.com

[1] Department of Anatomy, Faculty of Medicine, İzmir Kâtip Çelebi University, Balatçık Mah., Havaalanı Şosesi Cad., No: 33/2, 35620 Çiğli/İzmir, Turkey

ZA is a valuable element of the aesthetical or functional restoration of the face. Morphological details of the zygomatic bone and the ZA become essential for the reduction malarplasty (or zygomatic reduction) (Ma and Tang 2014; Smith and Grosse 2016; Song et al. 2009). Surgical devices may be placed medial to the space laterally bordered by ZA (Ma and Tang 2014; Song et al. 2009). For such reasons, the anatomical knowledge of not only the ZA but also the topographic anatomy of the temporal fossa is essential for surgical management (Song et al. 2009).

Despite the high success rates of the zygomaticus implants, this surgery necessitates advanced methods, and the complication risk is high. Landmarks on the frontal and temporal processes of the zygomatic bone are assessed for safer surgery during the placement of the zygomaticus implants (Takamaru et al. 2016). Presurgical anatomical evaluation of the zygomatic area is essential (Takamaru et al. 2016). Detailed morphometric anatomic descriptions of the ZA and TZS may increase the success of the surgery. However, in the literature, detailed morphometric and morphologic anatomic research reports regarding the ZA and TZS seem inadequate.

In human crania, less research has been carried out regarding the ZA. In the literature, relatively rare research reports discuss the developmental characteristics of the ZA and TZS (Usami and Itoh 2006). In adults, we could not reach such research reports describing the localization of the TZS on the ZA, joint shape type, and the suture margin pattern of TZS. This study is to describe the morphometric localization of the TZS on the ZA and morphological characteristics of the "joint shape type" and "suture margin pattern" of TZS aimed at dry adult human skulls.

Methods

In this research, the Western Anatolian dry human skulls from our anatomy laboratory's educational dry bone collection are evaluated. This research is approved by the Institutional Ethics Committee. Crania having deformed parts related to the planned research variables and measurements are excluded. For some crania, one side was excluded from the research due to the deformed parts, while the other side was not excluded. After this preliminary assessment, 32 crania were included in the research. Morphometric measurements were carried out bilaterally in 23 crania and unilaterally in 9 crania (right: 4, left: 5). A total of 55 TZSs were analyzed. There were no age or gender records of the bones. Each of the skulls was evaluated in terms of tooth eruption and general variables of the crania. All specimens were considered to belong to the adult age group (Manjunatha and Soni 2014).

General variables of the crania [head circumference (on glabella–opisthocranion plane), skull width (eurion–eurion), skull length (glabella–opisthocranion)] were measured directly by a measuring tape and a digital caliper according to the descriptions in the literature (Farkas et al. 1992, 1999). In digital images, indirect measurements (morphometric variables regarding the TZS and ZA) are performed with ImageJ software (Rasband, W.S., ImageJ, U. S. National Institutes of Health, Bethesda, Maryland, USA, https://imagej.nih.gov/ij/, 1997–2022). Then morphological features (classification/typology) were evaluated on dry bones and digital images of these bones.

Imaging technique

A tripod-mounted digital camera (Canon EOS 800D with a lens Canon EF-S 18–55 mm IS STM) was used to perform the imaging procedure. Skull position was standardized prior to imaging. While positioning the skull, appropriate anthropometric points were assessed on the anterior (norma anterior) and lateral (norma lateralis) views of the skulls.

Among the observable anthropometric points [vertex, nasion, nasospinale (supranasale), prosthion] in the norma anterior (anterior view), the appropriate ones were selected and aligned on the planum medianum (median plane) for vertical alignment of the skull. In the norma lateralis (lateral view), the Frankfurt line (porion–inferior margin of orbita) was used for the horizontal alignment of the skull according to the planum horizontale (horizontal plane). Photographs are taken from the lateral sides of the skulls perpendicular to the planum medianum (Fig. 1).

For the images for both sides, objective was placed 40 cm far away from the center of the ZA. The optic axis of the lens was set on the midline of ZA. It was set on the Frankfurt line. The optic axis was parallel to the planum horizontale (horizontal plane) and perpendicular to the planum medianum (medial plane). A ruler is placed next to the skulls during the photography to calibrate the measurements of images in the digital environment.

Morphometric measurements

During measurements using ImageJ software, pixel scale calibration is set up for each image analysis. Six "landmark lines" were determined on the photographs regarding the ZA and TZS (Fig. 1, Landmark lines: A–F). Eight morphometric variables are measured according to these landmarks (Fig. 1, Variables: #1–#8). There was no interobserver and intraobserver variability.
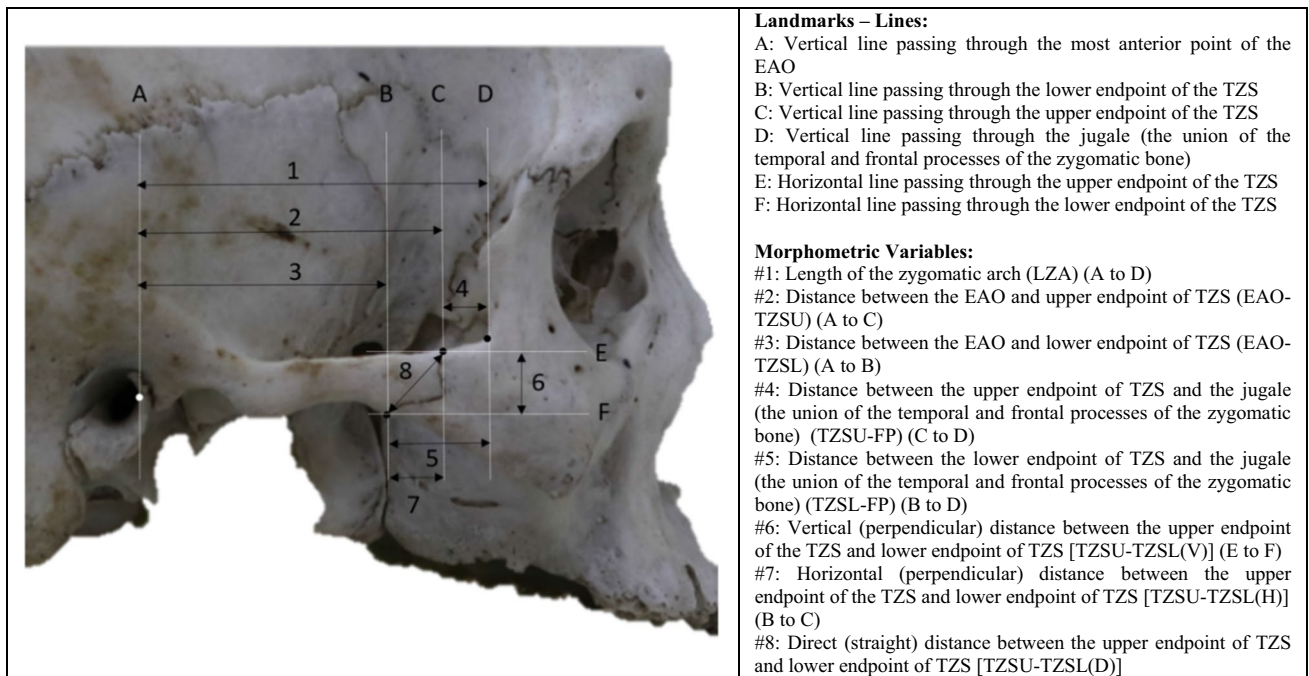
Landmarks – Lines:
A: Vertical line passing through the most anterior point of the EAO
B: Vertical line passing through the lower endpoint of the TZS
C: Vertical line passing through the upper endpoint of the TZS
D: Vertical line passing through the jugale (the union of the temporal and frontal processes of the zygomatic bone)
E: Horizontal line passing through the upper endpoint of the TZS
F: Horizontal line passing through the lower endpoint of the TZS

Morphometric Variables:
#1: Length of the zygomatic arch (LZA) (A to D)
#2: Distance between the EAO and upper endpoint of TZS (EAO-TZSU) (A to C)
#3: Distance between the EAO and lower endpoint of TZS (EAO-TZSL) (A to B)
#4: Distance between the upper endpoint of TZS and the jugale (the union of the temporal and frontal processes of the zygomatic bone) (TZSU-FP) (C to D)
#5: Distance between the lower endpoint of TZS and the jugale (the union of the temporal and frontal processes of the zygomatic bone) (TZSL-FP) (B to D)
#6: Vertical (perpendicular) distance between the upper endpoint of the TZS and lower endpoint of TZS [TZSU-TZSL(V)] (E to F)
#7: Horizontal (perpendicular) distance between the upper endpoint of the TZS and lower endpoint of TZS [TZSU-TZSL(H)] (B to C)
#8: Direct (straight) distance between the upper endpoint of TZS and lower endpoint of TZS [TZSU-TZSL(D)]

Fig. 1 Landmarks and the short descriptions of the morphometric variables of the zygomatic arch (ZA) and temporozygomatic suture (TZS). *EAO* external acoustic opening, *TZSU* upper endpoint of TZS, *TZSL* lower endpoint of TZS

Morphometric variables

#1 Length of the Zygomatic Arch (LZA): distance between the "Vertical line passing through the most anterior point of the External Acoustic Opening (EAO)" and "Vertical line passing through the jugale (the union of the temporal and frontal processes of the zygomatic bone)" (Fig. 1, variable #1, A–D).

#2 Distance between the EAO and upper endpoint of TZS(TZSU) (EAO-TZSU): distance between the "Vertical line passing through the anterior wall of the EAO" and "Vertical line passing through the upper endpoint of the TZS" (Fig. 1, variable #2, A–C).

#3 Distance between the EAO and lower endpoint of TZS(TZSL) (EAO-TZSL): distance between the "Vertical line passing through the anterior wall of the EAO" and "Vertical line passing through the lower endpoint of the TZS" (Fig. 1, variable #3, A–B).

#4 Distance between the upper endpoint of TZS (TZSU) and the jugale (the union of the temporal and frontal processes (FP) of the zygomatic bone) (TZSU-FP): distance between the "Vertical line passing through the upper endpoint of the TZS" and "Vertical line passing through the jugale (the union of the temporal and frontal processes of the zygomatic bone)" (Fig. 1, variable #4, C–D).

#5 Distance between the lower endpoint of TZS (TZSL) and the jugale (the union of the temporal and frontal processes (FP) of the zygomatic bone) (TZSL-FP): dis-
tance between the "Vertical line passing through the lower endpoint of the TZS" and "Vertical line passing through the jugale (the union of the temporal and frontal processes of the zygomatic bone)" (Fig. 1, variable #5, B–D).

#6 Vertical (V) (perpendicular) distance between the upper endpoint of the TZS and lower endpoint of TZS [TZSU-TZSL(V)]: distance between the "Horizontal line passing through the upper endpoint of the TZS" and "Horizontal line passing through the lower endpoint of the TZS" (Fig. 1, variable #6, E–F).

#7 Horizontal (H) (perpendicular) distance between the upper endpoint of the TZS and lower endpoint of TZS [TZSU-TZSL(H)]: distance between the "Vertical line passing through the lower endpoint of the TZS" and "Vertical line passing through the upper endpoint of the TZS" (Fig. 1, variable #7, B–C).

#8 Direct (D) (straight) distance between the upper endpoint of TZS and lower endpoint of TZS [TZSU-TZSL(D)] (Fig. 1, variable #8).

Morphological classification

TZSs were evaluated via the photographs and the skulls qualitatively. Two aspects of the TZSs were evaluated for the classification: (1) Joint shape type. (2) Suture margin pattern.

Determination of "joint shape type" of TZS

TZSs were examined in terms of shape and course to classify "joint shape types". During the first evaluation, remarkable joint shape types were noted according to the differences in shapes. The noted remarkable joint shape types were reviewed according to the principle of similarity. This step was repeated several times. Final joint shape types were determined based on the prominent shapes. Finally, TZSs were evaluated according to the final joint shape types and included in the appropriate class. The three researchers agreed on all shape types.

The "Joint shape" of TZS was defined in four different types (Fig. 2):

Type 1: angular type. Two lines create an angle.
Type 2: curvy type. The course is curved between the upper and lower endpoints of TZS.
Type 3: oblique type. A linear course. The upper endpoint of TZS is located more anteriorly than the lower endpoint of TZS. The vertical projection of the TZS is longer than the horizontal projection [TZSU-TZSL (V) > TZSU-TZSL (H)].

Type 4: horizontal type. A linear course. The upper endpoint of TZS is located more anteriorly than the lower endpoint of TZS. The vertical projection of the TZS is shorter than the horizontal projection [TZSU-TZSL (V) < TZSU-TZSL (H)].

Determination of the "suture margin pattern" of TZS

TZSs were examined regarding suturing patterns of the bony margins (contours) for the classification of "suture margin patterns". Remarkable suture margin patterns were noted according to the differences in patterns during the first evaluation. The noted remarkable suture margin patterns were reviewed according to the principle of similarity. This step was repeated several times. Final suture margin patterns were created based on the prominent patterns. Finally, TZSs were evaluated according to the final suture margin patterns and included in the appropriate class. The three researchers agreed on all shape types.

The "suture margins" of TZSs were defined in five different types (Fig. 3):
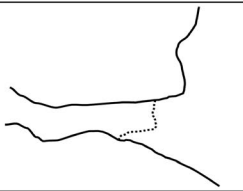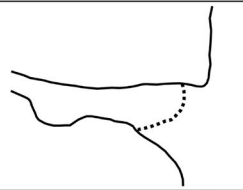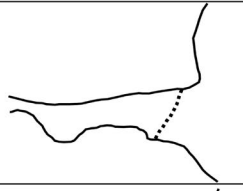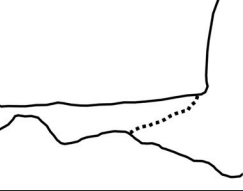
Type	Photo**	Sketch	Right* n (%)	Left* n (%)	Total n (%)
Type 1 (Angular)			10 (37.04)	9 (32.14)	19 (34.55)
Type 2 (Curvy)			7 (25.93)	12 (42.86)	19 (34.55)
Type 3 (Oblique)			5 (18.52)	3 (10.71)	8 (14.55)
Type 4 (Horizontal)			5 (18.52)	4 (14.29)	9 (16.36)
		Total	27 (100)	28 (100)	55 (100)

Fig. 2 Joint shape types of TZSs and the distribution of the subjects according to the lateralization [*n* (%)]. *Percentages calculated within columns, (Chi-square = 1.962, *df* = 3, *p* = 0.580)]. **Lateral views of the specimens on the right side
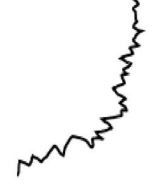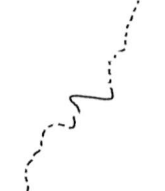
Type	Photo**	Sketch	Right* n (%)	Left* n (%)	Total* n (%)
Type A (Linear)			3 (11.11)	4 (14.29)	7 (12.73)
Type B (Denticulate)			10 (37.04)	9 (32.14)	19 (34.55)
Type C (Serrated)			8 (29.63)	5 (17.86)	13 (23.64)
Type D (Mixt)			4 (14.81)	8 (28.57)	12 (21.82)
Type E (Fused)			2 (7.41)	2 (7.14)	4 (7.27)
		Total	27 (100)	28 (100)	55 (100)

Fig. 3 Suture margin patterns of TZSs and the distribution of the subjects according to the lateralization [*n* (%)]. *Percentages calculated within columns, (Chi-square = 2.204, *df* = 4, *p* = 0.726)]. **Lateral views of the specimens on the right side

Type A: linear. The margins of the sutural surfaces articulate in the form of a straight line.

Type B: denticulate. The margins of the sutural surfaces articulate in the form of toothlike projections.

Type C: serrated. The margins of the sutural surfaces articulate in the form of saw-like projections.

Type D: mixt. Linear, denticulate, or serrated models are combined.

Type E: fused. The articular line is largely fused and indistinct.

Statistical analysis

SPSS Statistics Standard Concurrent User v25 (IBM Corp., Armonk, New York, USA) was used for statistical analysis. A *p* value of less than 0.05 was considered significant. The

distribution of data was evaluated using the Shapiro–Wilk test of normality. The mean values and standard deviations (SD) of the measurements were calculated. The minimum and maximum values were also presented where needed. Paired *T* test was used to compare the dependent groups, such as comparing the variables of the right side with ones on the left side of the crania. Pearson's correlation test was used to determine the correlation between the variables obtained. Descriptive statistics of the categorical data were calculated as percentages. The Chi-square test was used to compare the percentage distributions on sides.

Results

Morphometric variables

Descriptive statistics for the general variables of the crania (*n*: 32) were calculated; head circumference: 502.50 ± 17.56 mm, skull width: 120.34 ± 6.91 mm, and skull length: 161.22 ± 7.08 mm. Descriptive statistics of the morphometric variables describing the localization of the TZS on ZA are presented in Table 1.

All the morphometric variables could not be examined bilaterally in 32 skulls. Bilateral measurements were conducted on 23 skulls. The descriptive statistics of the variables for the crania, which are examined bilaterally, are presented in Table 2. In Table 2, findings of the statistical comparison of the sides were presented. On the left side, both the EAO-TZSU (#2) and EAO-TZSL (#3) values were

Table 1 Descriptive statistics of the morphometric variables describing the localization of the TZS on ZA on both sides (mm)

No.	Variables*	Left (*n*: 28)		Right (*n*: 27)	
		$\bar{x} \pm$ SD	Min–max	$\bar{x} \pm$ SD	Min–max
#1	LZA	47.10 ± 3.26	41.12–54.08	46.75 ± 3.25	40.30–52.45
#2	EAO-TZSU	42.88 ± 3.07	37.84–51.44	41.96 ± 3.42	34.83–50.45
#3	EAO-TZSL	34.53 ± 2.40	28.91–38.51	33.00 ± 3.26	27.17–39.94
#4	TZSU-FP	4.22 ± 1.70	1.19–7.94	4.79 ± 1.89	2.00–8.50
#5	TZSL-FP	12.53 ± 2.60	5.84–18.12	13.75 ± 2.49	8.49–18.63
#6	TZSU-TZSL (V)	10.42 ± 1.68	6.03–13.38	10.17 ± 1.52	7.11–12.22
#7	TZSU-TZSL (H)	8.35 ± 2.66	2.46–15.48	8.96 ± 2.34	4.28–16.63
#8	TZSU-TZSL (D)	13.35 ± 2.32	9.65–18.71	13.54 ± 2.14	9.99–20.04

$\bar{x}$ mean, *SD* standard deviation, *LZA* length of the zygomatic arch, *EAO* external acoustic opening, TZS temporozygomatic suture, *TZSU* upper endpoint of TZS, *TZSL* lower endpoint of TZS, *FP* frontal process of the zygomatic bone, *V* vertical, *H* horizontal, *D* direct

*Described in Fig. 1

Table 2 The descriptive statistics of the variables for the crania, which are examined bilaterally (L: 23, R: 23), and the statistical comparison of the sides (mm)

No.	Variables* (mm)	Sides		Test statistics	
		Left (*n*: 23) $\bar{x} \pm$ SD	Right (*n*: 23) $\bar{x} \pm$ SD	Test value	*p*
#1	LZA	47.84 ± 3.04	47.04 ± 3.07	$t = 1.844$	0.079
#2	EAO-TZSU	43.49 ± 2.94	42.46 ± 3.26	$t = 2.531$	0.019**
#3	EAO-TZSL	34.85 ± 2.32	33.38 ± 3.22	$t = 3.316$	0.003**
#4	TZSU-FP	4.34 ± 1.74	4.58 ± 1.81	$t = 0.712$	0.484
#5	TZSL-FP	12.96 ± 2.32	13.56 ± 2.42	$t = 1.734$	0.098
#6	TZSU-TZSL (V)	10.64 ± 1.69	10.22 ± 1.62	$t = 0.889$	0.073
#7	TZSU-TZSL (H)	8.64 ± 2.63	9.08 ± 2.50	$t = 0.192$	0.163
#8	TZSU-TZSL (D)	13.68 ± 2.33	13.60 ± 2.31	$t = 0.619$	0.744

$\bar{x}$ mean, *SD* standard deviation, *LZA* length of the zygomatic arch, *EAO* external acoustic opening, *TZS* temporozygomatic suture, *TZSU* upper endpoint of TZS, *TZSL* lower endpoint of TZS, *FP* frontal process of the zygomatic bone, *V* vertical, *H* horizontal, *D* direct

*Described in Fig. 1

**$p < 0.05$: statistically significant difference between the sides, *t* paired *t* test

Table 3 Correlation analysis and correlation coefficients of the morphometric variables (n: 23)

No.	Variables**	Side	#1		#2		#3		#4		#5		#6		#7		#8		#9	#10	#11
			L	R	L	R	L	R	L	R	L	R	L	R	L	R	L	R			
#1	LZA	L	1																		
		R	d^x	1																	
#2	EAO-TZSU	L	d^x	c^x	1																
		R	c^x	d^x	d^x	1															
#3	EAO-TZSL	L	c^x	c^x	c^y	c^y	1														
		R		c^x		d^x	d^x	1													
#4	TZSU-FP	L							1												
		R							c^{**}	1											
#5	TZSL-FP	L	c^x		c^y						1										
		R	b^z				$-b^{zn}$		b^z		d^x	1									
#6	TZSU-TZSL(V)	L											1								
		R											d^x	1							
#7	TZSU-TZSL(H)	L	b^z		c^x				$-b^{zn}$		d^x	c^y			b^z	1					
		R			c^y	b^z					c^x	c^x			d^x	1					
#8	TZSU-TZSL(D)	L			c^x						c^x	c^z	d^x	d^x	d^x	c^x	1				
		R			c^y						c^x	c^x	b^x	c^x	d^x	d^x	d^x	1			
#9	Skull circumference																		1		
#10	Skull width																		c^x	1	
#11	Skull length		b^z																d^x		1

LZA length of the zygomatic arch, *EAO* external acoustic opening, *TZS* temporozygomatic suture, *TZSU* upper endpoint of TZS, *TZSL* lower endpoint of TZS, *FP* frontal process of the zygomatic bone, *V* vertical, *H* horizontal, *D* direct, *L* left, *R* right

*Pearson correlation test

**Described in Fig. 1

$^x p < 0.001$, $^y p < 0.01$, $^z p < 0.05$, ^{n}Negative correlation, empty cells: no significant correlation

^{a}Correlation coefficient (*r*): 0.00–0.25

^{b}Correlation coefficient (*r*): 0.26–0.50

^{c}Correlation coefficient (*r*): 0.51–0.75

^{d}Correlation coefficient (*r*): 0.76–1.0

higher significantly than on the right side ($p < 0.05$, Table 2). No statistically significant differences were found for the other variables. The left LZA (#1) was longer than the right one. However, this difference was not significant.

Results of the correlation analysis are presented in Table 3 regarding the 23 crania, which are examined bilaterally. On both sides, positive correlational relationships are shown between the LZA (#1) and EAO-TZSU (#2) as well as between the LZA (#1) and EAO-TZSL (#3) (Table 3). While a significantly positive correlation was found between the left LZA (#1) and the skull length (#11) (Table 3), a significant correlation was not found between the right LZA (#1) and the skull length (#11) (Table 3).

Joint shape type

In each specimen, the upper endpoint of the TZS was located more anteriorly compared to the lower endpoint of TZS. Descriptive statistics as percentages and the sample images are presented in Fig. 2 regarding the "joint shape type". Each TZS was included in one of the type groups. Described types are Type 1 (angular), Type 2 (curvy), Type 3 (oblique) and Type 4 (horizontal). For all subjects (*n*: 55), the most frequent types were Type 1 (angular) (%34.55) and Type 2 (curvy) (%34.55). There was no significant association between the lateralization and the "joint shape types" (Chi-square = 1.962, *df* = 3, *p* = 0.580, Fig. 2).

Suture margin pattern

Descriptive statistics as percentages and the sample images are presented in Fig. 3 regarding the "suture margin patterns". Each TZS was included in one of the type groups. Described types are Type A (linear), Type B (denticulate), Type C (serrated), Type D (mixt) and Type E (fused). For all subjects (n: 55), the most frequent type was Type B (denticulate) (%34.55). There was no significant association

between the lateralization and the "suture margin pattern" (Chi-square = 2.204, df = 4, *p* = 0.726, Fig. 3).

Discussion

Sutures that connect the cranial bones consist of membrane-derived connective tissues (Adams 2016). Sutures serve as the growth sites for the cranium during postnatal growth (Niemann et al. 2021). Upon the completion of the growth, sutures convert to synostosis form. Interdigitated patterns are formed during the closure of the sutures, or sutures may completely be disappeared. In the literature, sutures are researched in humans and different primate species, focusing on the morphology and development of the sutures (Curtis et al. 2014). Morphology of the sutures is related to the intracranial or extracranial forces during the growth (Maloul et al. 2013). Structural characteristics of the sutures are examined under the biomechanical factors (Wang et al. 2012). These stress factors are researched in living humans or cadavers (Kim et al. 2015; Maloul et al. 2013).

In the literature, some researchers report that osteoclast resorption may affect the suture contour patterns (Byron 2006). In addition, some researchers examined suture closure with genetic factors (Opperman et al. 2006). Usually, rapid progression of the sutures is observed, while for some, obliteration does not occur even at an advanced age (Lynnerup and Jacobsen 2003).

Related to the technique, the surgeon may need metric information for the simulation and preparation of the surgical procedure or during the surgery to place the zygomatic implants (Takamaru et al. 2016). Similar to the ZA, TZS may be considered another landmark for surgical procedures concerning the pterion (Thunyacharoen and Mahakkanukrauh 2021). As well as the pterion, the marginal tubercle is another bony structure around the zygomatic arch to be evaluated in relation mini-pterional approach to the meningiomas (Aldahak et al. 2016). Morphologic landmarks such as the anterosuperior angle of the ZA are evaluated for locating the pterion for surgical purposes (Aksu et al. 2014). For such surgical approaches, on the ZA, TZS may give precise measurement/decision points as a more remarkable structure.

The shape and the projection of the zygomatic bone and the ZA affect the facial impression. The zygomatic bone is an essential structure in the form of the mid-facial anatomy. The morphological structure of the ZA is the consideration point for malarplasty and malar reduction surgery (Ma and Tang 2014; Smith and Grosse 2016; Song et al. 2009). During such procedures, the convexity of the zygomatic bone is reduced to narrow the facial width. As a morphometric consideration, geometric calculations may help the surgeon reduce the convexity of the ZA during the malarplasty ZA surgery (Ma and Tang 2014). Medially shifting the curvature

of the ZA by shaving the zygomatic process of the temporal bone is another surgical approach to intervene in the bony characteristics of the ZA (Lee 2016). During reduction malarplasty, precise sectioning is essential because asymmetrical osteotomies may result in facial asymmetry, which is an unwanted result (Kim et al. 2017). The asymmetrical structure of the face may result from the asymmetrical synostosis of TZS. (Manara et al. 2016; Rogers et al. 2007). While determining the osteotomy sites on the ZA, the localization and morphological features of the TZS may become essential. In addition, for safer surgical restoration for the fractures of the zygomatic bone and ZA, localization and morphological description of TZS may give valuable information. So, the asymmetrical potential of the regional bony structures such as TZS, which is in a close and casual relationship with the ZA might be essential while evaluating the clinical aspects.

Suture typing is one of the methods of forensic medicine to differentiate racial or geographic profiles (Gill 1995). Morphometric analysis of the digitally extracted models of the skulls is a modern approach for medicolegal purposes (Sholts et al. 2011). With the help of such methods, quantitatively analyzing the data of the coordinates of the sutures may help researchers statistically retrieve evidence to estimate the race and the geographic origin (Sholts and Wärmländer 2012). The success rates may be increased by evaluating the sutures quantitatively while classifying the skulls according to their geographic origin (Sholts and Wärmländer 2012). In their study, Sholts and Wärmländer (2012) classified the zygomaticomaxillary suture in digitalized 3D models. They demonstrated more successful results in differentiating the ethnic groups than the traditional classification. However, to our knowledge, no such reports indicate the methodological difference specific to TZS. Our research findings in the current report may provide preliminary findings in this field of research regarding the TZS. TZS may have a potential role with its closure time, 3D morphology, and racial, sexual, and age-related features like such sutures in the crania (Urban et al. 2016). In forensic medicine, decisions sometimes depend on the remnants of the skull. Therefore, any detail may become evidential information.

Fractal, in mathematics, is described as any of a class of complex geometric shapes that commonly have a "fractional dimension" (The Editors of Encyclopaedia Britannica 2022). Sutures may be presented in a fractal nature during the ossification of the cranial bones. Fractal geometric evidence may explain the differentiation during ontogenesis (Byron 2006; Wang et al. 2012). The bigger variation of the "fractal dimensions" reflects the complexity of the suture (Lynnerup and Jacobsen 2003). Therefore, fractal geometry can help researchers understand the quantitative morphology of sutures varying from linear types to highly convoluted types (Lynnerup and Jacobsen 2003; Yu et al. 2003). Fractal

geometry may discriminate the sex and race (Long and Long 1992; Lynnerup and Jacobsen 2003; Yu et al. 2003). To the best of our knowledge, this type of research on TZSs has not been carried out in the literature.

During the literature search, because we have not found any articles that present and discuss the findings of the morphological features of the TZS, a comparative discussion of the results of current research could not be presented. In our study, data were retrieved regarding the location of the TZS on ZA (Tables 1, 2). TZS was located in the anterior one-third of the ZA in each subject. Distances between the vertical line passing through the most anterior point of the EAO and the upper/lower endpoints of TZS (EAO-TZSU and EAO-TZSL, respectively) on the left side were significantly higher than those on the right side. Consistently with this finding, distances between the jugale and the upper/lower endpoints of the TZS on the left side were shorter than the equivalents on the right side. According to these findings, it is interpreted as TZS is located anteriorly on the left side. Consequently, considering the localization of the TZS, the length of the zygomatic process of the temporal bone and the temporal process of the zygomatic bone depend on the exact position of the TZS and differ. Because the cross-sectional design of our research, we avoid from commenting on the asymmetrical findings at a causal or evidential base. Craniofacial anomalies may result in asymmetry either on soft tissue or skeleton (Pagnoni et al. 2014). In addition, age, onset of the synostosis, progression of the development and race may affect the asymmetry (Rogers et al. 2007; Sholts and Wärmländer 2012).

TZS coursing roughly from superior to inferior and anterior to posterior in each specimen. Besides upper endpoint is located anteriorly compared to the lower endpoint. Three variables representing the dimensions of the TZS were evaluated. These are the vertical [TZSU-TZSL (V)], horizontal [TZSU-TZSL (H)], and oblique [TZSU-TZSL (D)] projections of the TZS (Fig. 1). The vertical projection (TZSU-TZSL-V) of the TZS was statistically higher than the horizontal [TZSU-TZSL (H)] projection ($p < 0.05$). These secondary findings may reflect the asymmetrical positioning of the TZS and may be considered in association with reconstructive or aesthetic surgery.

Except for the significant correlation between the skull length and the left LZA, there was no significant correlation between the general skull variables (head circumference, skull width, skull length) and the morphometric variables of the TZS and ZA. It was interpreted as the location and dimensions of the TZS may be examined regardless of the cranial dimensions. LZA may be palpated and measured in living humans. Variables significantly correlated with the LZA may be evaluated by the clinician non-invasively. However, regression analysis was not carried out due to the small sample size of the subjects.

To the best of our knowledge, in this research, detailed information and classification of the joint type and suture margin pattern of the TZS are reported for the first time. In this aspect, our findings may be interpreted as preliminary data regarding the TZS in terms of both descriptions and the distribution of the samples. On both sides of the crania, angular and curvy types were the most frequent joint shape types in the four types (Fig. 2). The denticulate and serrated types were the most frequent suture margin patterns (Fig. 3). Our results suggest no statistically significant relation between the lateralization and distribution of classifications. Categorical data analysis is interpreted as there were no significant differences between the sides in terms of both "joint shape type" and "suture margin pattern" (Figs. 2, 3). Our results showed that the linear and fused types (13% and 7%, respectively. Figure 3) of suture margin patterns have a considerable percentage in the crania. These types of suture margin patterns may make it difficult estimation for medicolegal purposes.

Providing detailed data on morphological and morphometric features regarding the cranial sutures may enhance the success of surgical procedures. Further research seems required in the field of suture morphology (Lynnerup and Jacobsen 2003). The classification described in our report may be evaluated in further research while comparing the racial characteristics of the crania.

This research has some limitations. This research is conducted on a relatively smaller number of crania in a single institution. We do not have the demographic records of the skulls (i.e., age, sex, and postmortem duration). In the literature, there are some methods used to predict the gender or exact age of the skeletal remnants, which may still have aspects that can be criticized by some researchers. So, in terms of the structural base of our research, we haven't preferred to predict the age or genders due to our research is not established on the age or gender variability. It is based on the basic morphological features of the TZS. Further research may be needed to generalize the findings of this research. The surface features of the TZSs were classified qualitatively in this research. Due to the subjectivity of the qualitative classification, further quantitative, three-dimensional, or histological analyses may be needed to understand the detailed structure of the TZS.

For further research, TZS can be evaluated in respect to different age groups (young, middle age, old) or different medical history features (different pathological or physiological conditions). Because any conditions on the bony development throughout the life may have potential effects on the TZS morphology. Unfortunately, we had to ignore such factors.

In conclusion, this research aimed to evaluate the localization and morphological features of the TZS. To the best of our knowledge, the current article is the first report

discussing the morphological findings of TZS in adult humans. We believe this can be considered a strong aspect of this research. Despite the limitations, preliminary data were retrieved in this field of research. Current findings revealed that the left TZS was more anterior than the right side. No significant relation was found between the lateralization and the morphological types. Concerning the morphometric variables, the significant differences between the sides and the nonsignificant correlations suggest an asymmetrical structure. Detailed anatomical and personalized evaluation of the TZS seem essential for clinicians' regional medical and surgical approaches.

Declarations

References

Adams MA (2016) Functional anatomy of the musculoskeletal system. In: Standring S (ed) Gray's anatomy: the anatomical basis of clinical practice. Elsevier Limited, Philadelphia, pp 81–123

Aksu F, Akyer SP, Kale A, Geylan S, Gayretli O (2014) The localization and morphology of pterion in adult west Anatolian skulls. J Craniofac Surg 25:1488–1491. https://doi.org/10.1097/scs.0000000000000790

Aldahak N, El Tantowy M, Dupre D et al (2016) Drilling of the marginal tubercle to enhance exposure via mini pterional approach: an anatomical study and clinical series of 25 sphenoid wing meningiomas. Surg Neurol Int 7:989–994. https://doi.org/10.4103/2152-7806.195575

Byron CD (2006) Role of the osteoclast in cranial suture waveform patterning. Anat Rec 288A:552–563. https://doi.org/10.1002/ar.a.20322

Cui Y, Leclercq S (2017) Environment-related variation in the human mid-face. Anat Rec 300:238–250. https://doi.org/10.1002/ar.23467

Curtis N, Witzel U, Fagan MJ (2014) Development and three-dimensional morphology of the zygomaticotemporal suture in primate skulls. Folia Primatol 85:77–87. https://doi.org/10.1159/000357526

Farkas LG, Posnick JC, Hreczko TM (1992) Anthropometric growth study of the head. Cleft Palate Craniofac J 29:303–308. https://doi.org/10.1597/1545-1569_1992_029_0303_agsoth_2.3.co_2

Farkas LG, Tompson B, Phillips JH, Katic MJ, Cornfoot ML (1999) Comparison of anthropometric and cephalometric measurements of the adult face. J Craniofac Surg 10:18–25. https://doi.org/10.1097/00001665-199901000-00005

Gill GW (1995) Challenge on the frontier: discerning American Indians from whites osteologically. J Foren Sci 40:783–788. https://doi.org/10.1520/JFS15384J

Gleeson M (2016) Head and neck. In: Standring S (ed) Gray's anatomy: the anatomical basis of clinical practice. Elsevier Limited, Philadelphia, pp 416–428

Kim KY, Bayome M, Park JH, Kim KB, Mo SS, Kook YA (2015) Displacement and stress distribution of the maxillofacial complex during maxillary protraction with buccal versus palatal plates: finite element analysis. Eur J Orthodont 37:275–283. https://doi.org/10.1093/ejo/cju039

Kim HL, Kwon JS, Choi YJ, Lee UL (2017) A three-dimensional planned osteotomy on the zygomatic arch for reduction malarplasty. Int J Oral Maxillofac Surg 46:1024–1025. https://doi.org/10.1016/j.ijom.2017.03.014

Lee TS (2016) The importance of shaving the zygomatic process during reduction malarplasty. Int J Oral Maxillofac Surg 45:1002–1005. https://doi.org/10.1016/j.ijom.2016.01.001

Long CA, Long JE (1992) Fractal dimensions of cranial sutures and waveforms. Acta Anat 145:201–206. https://doi.org/10.1159/000147366

Lynnerup N, Jacobsen JC (2003) Brief communication: age and fractal dimensions of human sagittal and coronal sutures. Am J Phys Anthropol 121:332–336. https://doi.org/10.1002/ajpa.10260

Ma F, Tang S (2014) Zygomatic arch reduction and malarplasty with multiple osteotomies: its geometric considerations. Aesthetic Plast Surg 38:1143–1150. https://doi.org/10.1007/s00266-014-0405-4

Maloul A, Fialkov J, Whyne CM (2013) Characterization of the bending strength of craniofacial sutures. J Biomech 46:912–917. https://doi.org/10.1016/j.jbiomech.2012.12.016

Manara R, Schifano G, Brotto D et al (2016) Facial asymmetry quantitative evaluation in oculoauriculovertebral spectrum. Clin Oral Investig 20:219–225. https://doi.org/10.1007/s00784-015-1660-8

Manjunatha BS, Soni NK (2014) Estimation of age from development and eruption of teeth. J Foren Dent Sci. 6(2):73–76. https://doi.org/10.4103/0975-1475.132526

Niemann K, Lazarus L, Rennie CO (2021) Developmental changes of the facial skeleton from birth to 18 years within a South African cohort (a computed tomography study). J Foren Leg Med 83:102243. https://doi.org/10.1016/j.jflm.2021.102243

Opperman LA, Fernandez CR, So S, Rawlins JT (2006) Erk1/2 signalling is required for TGF-beta 2-induced suture closure. Dev Dyn 235:1292–1299. https://doi.org/10.1002/dvdy.20656

Pagnoni M, Fadda MT, Cascone P, Iannetti G (2014) A novel osteogenic distraction device for the transversal correction of temporozygomatic hypoplasia. J Cranio-Maxillo Fac Surg 42:616–622. https://doi.org/10.1016/j.jcms.2013.09.002

Rogers GF, Greene AK, Oh AK, Robson C, Mulliken JB (2007) Zygomaticotemporal synostosis: a rare cause of progressive facial asymmetry. Cleft Palate Craniofac J 44:106–111. https://doi.org/10.1597/05-148

Sholts SB, Wärmländer SK (2012) Zygomaticomaxillary suture shape analyzed with digital morphometrics: reassessing patterns of variation in American Indian and European populations. Foren Sci Int 217:234.e1-234.e6. https://doi.org/10.1016/j.forsciint.2011.11.016

Sholts SB, Walker PL, Kuzminsky SC, Miller KW, Wärmländer SK (2011) Identification of group affinity from cross-sectional contours of the human midfacial skeleton using digital morphometrics and 3d laser scanning technology. J Foren Sci 56:333–338. https://doi.org/10.1111/j.1556-4029.2011.01701.x

Smith AL, Grosse IR (2016) The biomechanics of zygomatic arch shape. Anat Rec 299:1734–1752. https://doi.org/10.1002/ar.23484

Song WC, Choi HG, Kim SH et al (2009) Topographic anatomy of the zygomatic arch and temporal fossa: a cadaveric study. J Plast

Reconstr Aesthet Surg 62:1375–1378. https://doi.org/10.1016/j.bjps.2008.06.037

Takamaru N, Nagai H, Ohe G et al (2016) Measurement of the zygomatic bone and pilot hole technique for safer insertion of zygomaticus implants. Int J Oral Maxillofac Surg 45:104–109. https://doi.org/10.1016/j.ijom.2015.07.015

The Editors of Encyclopaedia Britannica. (2022) Fractal [Web Page]. Encyclopaedia Britannica. Available: https://www.britannica.com/science/fractal. Accessed 26 Mau 2022

Thunyacharoen S, Mahakkanukrauh P (2021) Anatomical variations and morphometric study of pterion in a Thai population associated with clinical implications. Int J Morphol 39:1048–1053. https://doi.org/10.4067/S0717-95022021000401048

Urban JE, Weaver AA, Lillie EM, Maldjian JA, Whitlow CT, Stitzel JD (2016) Evaluation of morphological changes in the adult skull with age and sex. J Anat 229:838–846. https://doi.org/10.1111/joa.12247

Usami A, Itoh I (2006) Morphological changes in the zygomatic arch during growth. Pediatr Dent J 16:179–183. https://doi.org/10.1016/s0917-2394(06)70084-2

Wang Q, Wood SA, Grosse IR et al (2012) The role of the sutures in biomechanical dynamic simulation of a macaque cranial finite element model: implications for the evolution of craniofacial form. Anat Rec 295:278–288. https://doi.org/10.1002/ar.21532

Yu JC, Wright RL, Williamson MA, Braselton J, Abell ML (2003) A fractal analysis of human cranial sutures. Cleft Palate Craniofac J 40:409–415. https://doi.org/10.1597/1545-1569(2003)040%3c0409:afaohc%3e2.0.co;2